PHOTONICS Research

High efficiency solid–liquid hybrid-state quantum dot light-emitting diodes

Jia-Sheng Li,[1,2] Yong Tang,[1] Zong-Tao Li,[1,2,*] Long-Shi Rao,[1] Xin-Rui Ding,[1] and Bin-Hai Yu[1]

[1]Engineering Research Center of Green Manufacturing for Energy-Saving and New-Energy Technology, South China University of Technology, Guangzhou 510640, China
[2]Foshan Nationstar Optoelectronics Company Ltd., Foshan 528000, China
*Corresponding author: meztli@scut.edu.cn

Received 8 August 2018; revised 9 October 2018; accepted 10 October 2018; posted 12 October 2018 (Doc. ID 341874); published 14 November 2018

Quantum dots (QDs) can achieve high quantum yields close to unity in liquid solutions, whereas they exhibit a decreased conversion efficiency after being integrated into solid-state polymer matrices for light-emitting diode (LED) devices, which is called the host matrix effect. In this study, we propose a solid–liquid hybrid-state QD-LED to solve this issue. The ethylene-terminated polydimethylsiloxane (ethylene-PDMS) is used to establish a solid-state cross-linked network, whereas the methyl-terminated PDMS (methyl-PDMS) is used in its liquid state. From a macroscopic level, the cured solid–liquid hybrid-state PDMS (SLHP) composites reach a solid state, which is stable and flexible enough to be used in LED devices. Compared with LEDs using conventional QD/solid PDMS composites at equal color conversion efficiency ranging from 40% to 60%, the luminous flux of LEDs with QD/SLHP composites is increased by 13.0% using an optimized methyl-PDMS concentration of 85 wt. %. As a result, high efficiency QD-LEDs using QDs as the only color convertor with luminous efficacy of 89.6 lm/W (0.19 A) were achieved, which show a working stability comparable with that using conventional solid-state structures at a harsh condition. Consequently, the novel approach shows great potential for achieving high efficiency and high stability QD-LEDs, which is also compatible with current structures used in illumination and display applications.

https://doi.org/10.1364/PRJ.6.001107

1. INTRODUCTION

Quantum dots (QDs) exhibit high quantum yields (QYs) and narrow emission spectra and are easy to produce [1]. Thus, they show great potential for optoelectronic devices requiring color conversion functions[2,3], such as light-emitting diodes (LEDs) [4]. Much effort is devoted to improving the QYs of QDs by optimizing the synthetic methods [5] and band structures [6]. At present, CdSe/ZnS QDs with core/shell structures achieve a QY of above 90% [1,7] and have become one of the most promising color conversion materials to replace conventional rare-earth-based phosphors in LEDs [8,9] for illumination and display applications. LEDs need packaging processes [10–12] in which the QDs are sealed in transparent polymer matrices to protect them from environmental-moisture-induced oxidation [13]. After the QDs have been fabricated in oily or water solutions [5,14], they must be transferred to a polymer matrix before being used in LED packaging to prevent the solution from accelerating the degradation of the LED chips and other packaging elements, such as the lead frame and encapsulant [10,15]. However, the conversion efficiency of large QD quantities in a polymer matrix is far lower than that in a solution [16] owing to reabsorption loss [17,18], aggregation-induced quenching [19,20], and improper interactions with the polymer matrix [21,22], which is also called the host matrix effect. Thus, the luminous efficacy of QD-LEDs is much poorer than that of conventional phosphor-based LEDs [18], thereby suppressing commercial applications of QD-LEDs.

To improve their optical performance, much effort has been devoted to the optimization of their polymer matrices [16,23–27]. For instance, polydimethylsiloxane (PDMS), which exhibits good flexibility, high transparency, and simple manufacture, provides good dispersity and compatibility for oil-soluble QDs and has been widely employed for QD-LED packaging [13,22,28–32]. Thus far, the luminous efficacy of LEDs with QD/solid PDMS (SP) composites is still far lower than that of LEDs with QDs in original solutions [33–35]. The original liquid-state solution provides a better environment for dispersed QDs and ensures a high optical LED performance, which leads to a record performance of 105 lm/W (injection current of 10 mA) for QD-LEDs using green QDs in the liquid state as the only color convertor [35]. However, this liquid

solution also creates an obstacle for LED devices due to their limitations of unfixed shape, toxicity, volatility, high corrosivity to packaging elements, and ease of leakage. Also, it is difficult to achieve stable and flexible QD films for backlight applications [36].

In this paper, we propose a high efficiency solid–liquid hybrid-state QD-LED. The methyl-terminated PDMS (methyl-PDMS) and the ethylene-terminated PDMS (ethylene-PDMS) were combined; owing to the interaction with a curing agent, the ethylene-PDMS became cross-linked and provided a solid-state network for the storage of liquid methyl-PDMS. This novel approach shows great potential for achieving high efficiency and high stability QD-LEDs, which are also compatible with current structures used in illumination and display applications.

2. EXPERIMENTS

A. Materials

The oil-soluble green CdSe/ZnS QDs with core/shell structure were purchased from China Beijing Beida Jubang Science & Technology Co., Ltd. (QY of 90%, emission peak at 520 nm). The methyl-PDMS, ethylene-PDMS, and curing agent were purchased from Dow Corning. The encapsulant M-2815 was purchased from Shenzhen Jindi Electronic Materials Co., Ltd.; chloroform solution from Aladdin Reagents Co., Ltd.; and blue LED devices from Foshan NationStar Optoelectronics Co., Ltd. (emission wavelength centered at 455 nm). All chemicals were used directly without further purification.

B. Fabrication Method

First, QDs were added to a 1.5 mL chloroform solution. The QD masses ranged from 2 to 16 mg to control the QD concentration in the polymer matrix. Then, the methyl-PDMS, ethylene-PDMS, and curing agent were added to the QD solution. The total mass of these polymers was kept at 2000 mg, and the ratio of methyl-PDMS mass to total mass ranged from 0 to 90 wt. %. The mixture was stirred for 50 min in the planetary stirring machine with vacuum treatment to uniformly disperse the QDs in the polymer matrix by evaporating the chloroform solution and removing the bubbles. The resulting composites were dispensed onto the lead frame of the blue LED devices; the dispensed mass weighed 3.0 mg. The composite-filled blue LED devices were heated in an oven at 125°C for 90 min to cure the composites. After that, a spherical lens was added to each LED device, and the encapsulant was filled inside the lens to improve light extraction. Finally, the LED devices were heated in the oven at 120°C for 15 min to cure the encapsulant.

The fabrication processes of the composites for QD films were the same as those of the devices. However, the composites were injected into the mold instead of the device. Similarly, the composite-injected mold was heated in the oven at 125°C for 90 min. After the heat curing, the composites were removed from the mold and flexible QD films were obtained.

C. Characterizations

The optical performances of QD-LEDs—including their radiant power, luminous flux, and spectra—were measured with integrating-sphere systems from Instrument Systems GmbH. The LED injection current of 0.19 A was controlled by a Keithley SourceMeter. The optical properties of the films, including transmittance, reflection, haze, and absorption, were measured with a dual-beam UV-Vis spectrophotometer TU-1901 from Beijing Persee General Instrument Co., Ltd. The infrared transmittance spectra were measured with a Fourier transform infrared spectrometer from Bruker.

3. PRINCIPLE

A. Realization of Solid–Liquid Hybrid State

Solid-state QD/polymer composites are required to achieve a high stability for illumination and display applications [33,36]. First, we investigated the maximum concentration of methyl-PDMS to ensure that the ethylene-PDMS can be entirely cross-linked to create a network and achieve its solid state after curing. The QD/SLHP composites with methyl-PDMS concentrations of 80 wt. %, 85 wt. %, and 90 wt. % after curing at 125°C for 90 min are shown in Fig. 1(a) under ultraviolet irradiation. Please note that the containers were inverted to conveniently observe the composite fluidity. The composites gained with methyl-PDMS concentrations below 85 wt. % are accumulated at the container bottoms. However, those gained with methyl-PDMS concentrations of 90 wt. % cannot

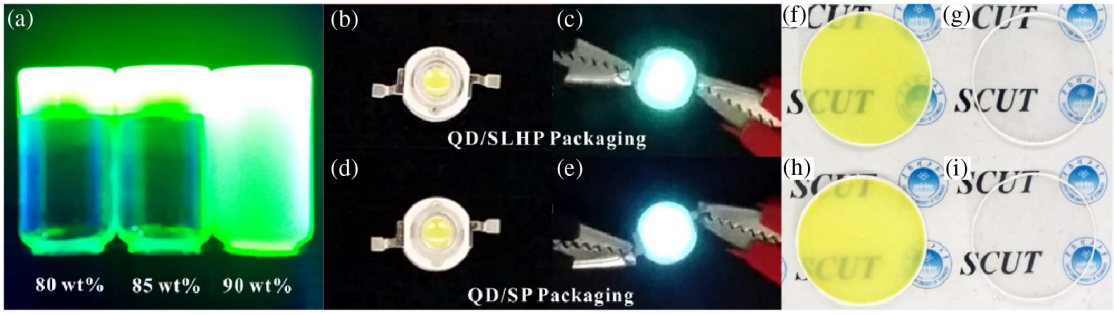

Fig. 1. (a) SLHP with methyl-PDMS concentrations of 80 wt. %, 85 wt. %, and 90 wt. % after curing at 125°C for 90 min, respectively. (b)–(c) LED images with QD/SLHP packaging structure (concentrations of QDs and methyl-PDMS are 0.8 and 85 wt. %, respectively) under injection currents of 0 and 2 mA, respectively. (d)–(e) LED images with QD/SP packaging structure (concentrations of QDs and methyl-PDMS are 0.8 and 0, respectively) under injection currents of 0 and 2 mA, respectively. Images of (f) QD/SP film (0.3 wt. % QDs), (g) SP film, (h) QD/SLHP film (0.3 wt. % QD and 85 wt. % methyl-PDMS), and (i) SLHP film (85 wt. % methyl-PDMS).

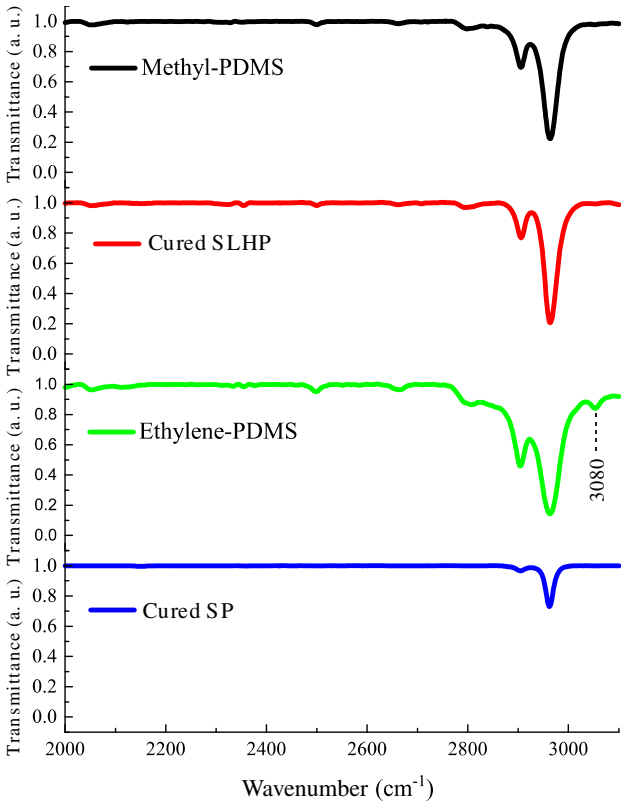

Fig. 2. Infrared transmittance spectra of methyl-PDMS, ethylene-PDMS, cured SP, and cured SLHP with 15 wt. % methyl-PDMS.

turn into the solid state and flow along the container wall. Therefore, the maximum methyl-PDMS concentration was set to 85 wt. % for subsequent investigations. To verify that ethylene-PDMS can be cross-linked when combined with methyl-PDMS and that methyl-PDMS can exist in its original liquid state in cross-linked networks of ethylene-PDMS, the infrared transmittance spectra of methyl-PDMS, ethylene-PDMS, cured ethylene-PDMS (SP), and cured composites of ethylene-PDMS with 15 wt. % of methyl-PDMS [solid–liquid hybrid-state PDMS (SLHP)] are given in Fig. 2. The absorption peak at 3080 cm^{-1} of ethylene-PDMS is due to the C=C bond located at the terminated ethylene [37]. After the interaction with the curing agent that includes a polymer chain with Si–H groups, the ethylene-PDMS is cross-linked according to the hydrosilylation reaction between Si–H and C=C bonds. Therefore, the absorption peak of C=C bonds does not appear for solid PDMS. Regarding SLHP, the absorption peak of the C=C bonds also does not exist in the infrared transmittance spectra. This clearly demonstrates that the hydrosilylation reaction of ethylene-PDMS has been entirely completed even with added methyl-PDMS. Thereby, solid-state cross-linked networks can be produced. Moreover, the characteristic peaks of the SLHP are approximately equal to those of methyl-PDMS. Consequently, the SLHP contains a great amount of the original liquid methyl-PDMS in its networks because the methyl-PDMS did not participate in the reaction and thus provides a liquid-state environment for the QDs.

B. Effect of Liquid-Type Methyl-PDMS on QDs

The QD-LEDs and films have been fabricated to investigate the effect of liquid-type methyl-PDMS on QDs. First, LEDs with the conventional SP packaging structure were used for comparison. Their samples can be seen in Figs. 1(b)–1(e); please note that the packaging geometries are equal. According to previous studies, QDs in liquid solutions where they are originally synthesized exhibit a higher conversion efficiency [16,34,35] than those in solid-state polymer matrices. Here, we found that the liquid-type methyl-PDMS can also contribute to a high efficiency for QDs. The optical performance of QD-LEDs with different methyl-PDMS concentrations is given in Fig. 3. Their total radiant power exhibits approximately no change, whereas the luminous flux obviously increases with increasing methyl-PDMS concentration. Thus, much more QD light (light emission from QDs) is generated by the QDs, increasing the green-light proportion, which is more sensitive to the luminosity function of the human eye [38]. One reasonable explanation is that the introduction of methyl-PDMS in ethylene-PDMS networks can provide a flexible environment for QDs, thereby preventing the increase of surface defects.

As the infrared transmittance spectrum of QDs shows in Fig. 4, the absorption peaks at 1280, 1462, and 1710 cm^{-1} exhibit the presences of C–O stretch, O–H stretch, and C=O stretch, respectively. This indicates that the oil-soluble QDs have oleic acid ligands on their surface. As shown in the diagram of Fig. 5, the C=C bonds of these ligands can also

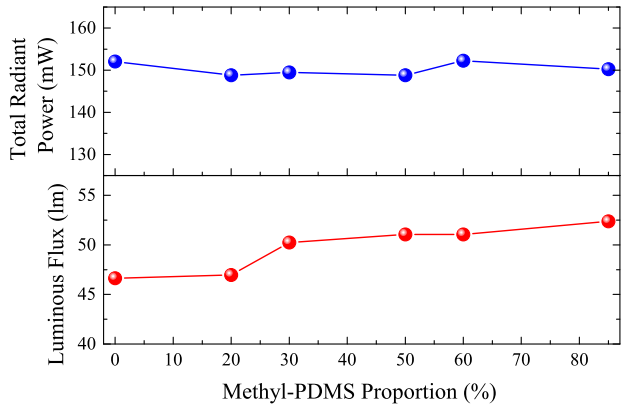

Fig. 3. Total radiant power and luminous flux of LEDs with QD/SLHP composites for different methyl-PDMS concentrations; the QD concentration is kept at 0.6 wt. %.

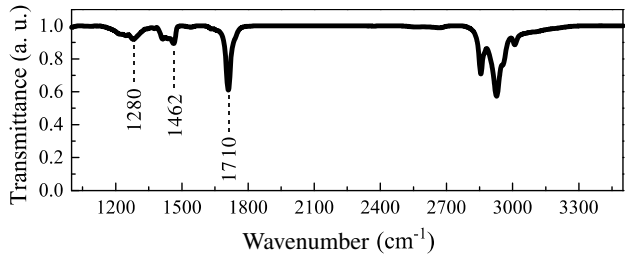

Fig. 4. Infrared transmittance spectrum of CdSe/ZnS QDs.

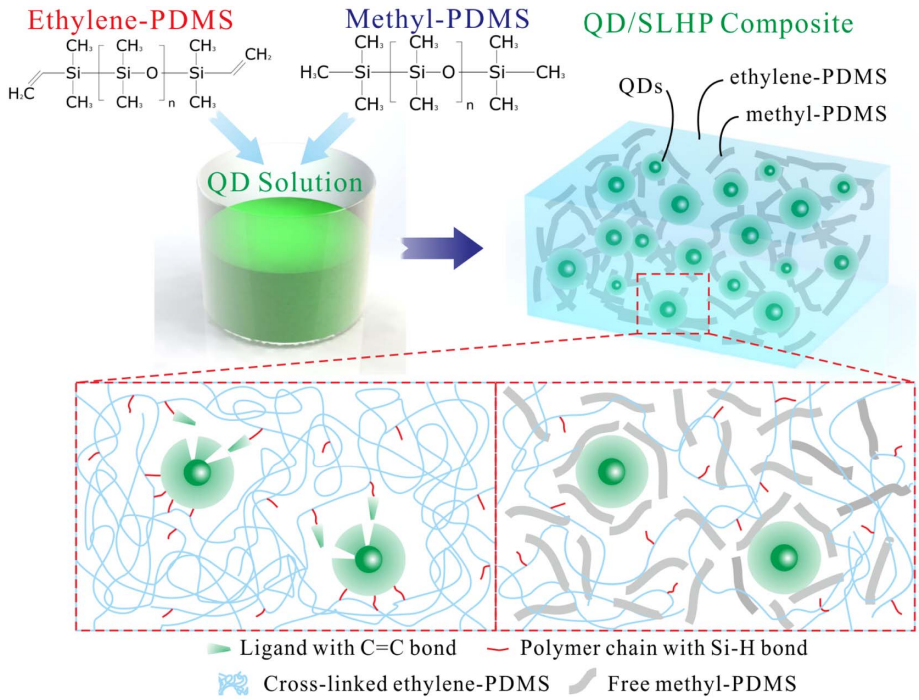

Fig. 5. Fabrication method for QD/SLHP composites. The liquid methyl-PDMS provides a flexible environment to prevent ligands on QD surfaces from being dragged away by the cross-linked ethylene-PDMS network.

interact with the Si–H bonds of the ethylene-PDMS networks [22]. Since the ethylene-PDMS networks possess a relatively high rigidity owing to the cross-linking, the polymer chains with Si–H bonds of the cross-linked networks have difficulties reaching the QDs under the chemical force induced by the Si–H bonds of the networks and the C=C bonds of the ligands. By contrast, free QDs can actively reach the cross-linked networks under this chemical force and complete the hydrosilylation reaction. However, many ligands reside on a QD surface and have a high probability to interact with the network at different locations. Since the Si–C bonds between networks and ligands are stronger than the Zn–O bonds between QDs and ligands, the ligands can be removed from QDs by the pulling network, thereby causing more surface defects on QDs. With increasing methyl-PDMS concentration, more QDs can be freely excited in the liquid environment with high flexibility, preventing the ligands from being drawn away by the networks with relatively high rigidity. QDs with less surface defects can lead to less nonradiative recombinations, resulting in more QD light in the QD-LEDs with higher methyl-PDMS concentrations. The other possible reason is that an increasing amount of methyl-PDMS with low kinematic viscosity (in this study, 500 m^2/s) is beneficial to decrease the system viscosity of the SLHP composites during QD dispersion [22]. In other words, a larger methyl-PDMS concentration helps prevent QD aggregation and sedimentation in the composites, guaranteeing many more QDs to be excited by the chip light (light emission from LED chips) in LEDs.

The QD/SP films, SP films, QD/SLHP films, and SLHP films were fabricated to further verify the effect of SLHP composites on QDs. Their samples are shown in Figs. 1(f)–1(i), respectively. The transmittance, haze, absorption, and reflection spectra of the SP film and SLHP film (with 85 wt. % methyl-PDMS) are shown in Fig. 6(a). Both films exhibit transmittance values of 93% and low absorption and reflection. Besides, the haze of the SLHP film is higher than that of the SP film, indicating that the SLHP film has a stronger scattering ability for visible light. This may be caused by the interfaces introduced by methyl-PDMS inside the cross-linked ethylene-PDMS network. However, both haze values are below 3%. The slight difference can be neglected after their interactions with QDs. The absorption spectra of QD/SLHP films (85 wt. % methyl-PDMS) and QD/SP films with QD concentrations of 0.3 wt. %, 0.5 wt. %, and 0.8 wt. % are shown in Figs. 6(b)–6(d), respectively. Regarding the chip spectra, the absorption of the QD/SLHP film is higher than that of the QD/SP film; this is mainly caused by the lower viscosity of methyl-PDMS during QDs dispersion, which results in a greater QD amount in the SLHP composites. However, the QD/SLHP film has a lower absorption in the QD spectra and an even longer wavelength of above 600 nm. To compare the absorption spectra at long wavelengths, they are normalized to the chip wavelength for convenience. Evidently, the QD/SP film has a stronger absorption ability for long wavelengths than the QD/SLHP film. Moreover, the differences in the absorption for long wavelengths between the QD/SLHP film and QD/SP film become more significant as the QD concentration increases. Since the defect states in the midgap of the QDs compete to capture long-wavelength photons with low energies [39,40], the results further support that SLHP composites protect the ligands of QDs, reducing the defect states.

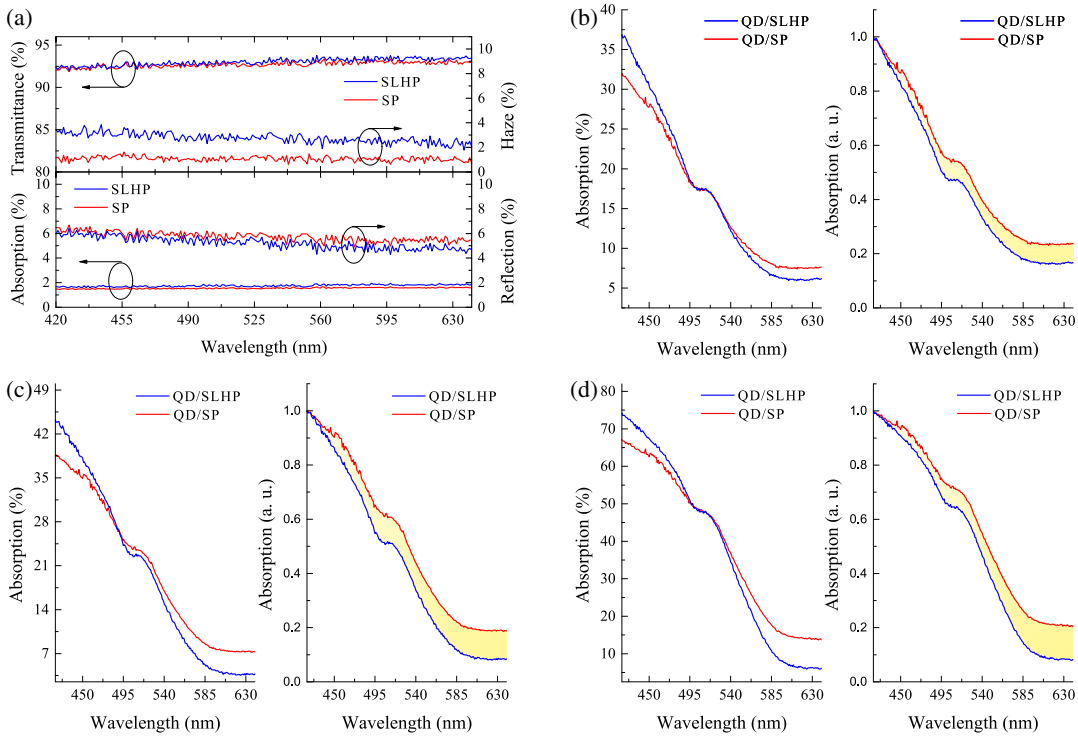

Fig. 6. (a) Transmittance, haze, absorption, and reflection spectra of SP film and SLHP film (with 85 wt. % methyl-PDMS). (b)–(d) Absorption spectra of QD/SP film and QD/SLHP film with QD concentrations of 0.3 wt. %, 0.5 wt. %, and 0.8 wt. %, respectively.

4. OPTICAL PERFORMANCES OF QD-LED

A. Light Efficiency

The optical performances of QD-LEDs with different QD concentrations are given. Figure 7(a) shows the total radiant power and luminous flux of QD-LEDs with QD/SLHP composites and QD/SP composites with QD concentrations from 0.1 wt. % to 0.8 wt. %, respectively. Both total radiant power values decrease with increasing QD concentration owing to the increased reabsorption loss between QDs [17]. The total radiant power values under equal QD concentrations show approximately no difference, indicating an equal optical power loss in these two LED types. Evidently, QD/SLHP composites are beneficial to gain a higher luminous flux in LEDs with different QD concentrations. For further investigations, the radiant-power values of the chip light and QD light were separated from the total radiant power values by integrating the blue and green spectra, respectively, as shown in Fig. 7(b). The radiant power of the chip light from QD/SLHP composites is lower than that from QD/SP composites under different QD concentrations. Thus, the QDs in the QD/SLHP composites absorbed more chip light. This confirms that QD/SLHP composites with lower viscosity can provide a better dispersity for QDs, preventing their aggregation and sedimentation in the composites without being excited by chip light. As a result, a higher radiant power in the QD light can be observed for LEDs with QD/SLHP composites. Most importantly, the high amount of chip light absorbed by QDs also indicates that much more color conversion events occurred. This can generally lead to a lower total radiant power owing to nonradiative recombinations [18,41]. However, the total radiant power gained by QD/SLHP composites is still equal to that gained by QD/SP composites, as discussed above. Hence, the conversion loss of a single QD in SLHP composites can be lower than that in SP composites.

It is more reasonable to compare the optical performances of both LED types under equal QD light proportion. The color conversion efficiency (CCE) (the ratio of QD light radiant power to the system) can characterize the QD light proportion and output color of LEDs, which is generally used as a constant condition for the comparison of LED performances [31,38], as shown in Fig. 7(c). Owing to the higher quantity of generated QD light in SLHP composites, the CCE gained with QD/SLHP composites is higher than that gained with QD/SP composites. At equal CCEs, both total radiant power and luminous flux of LEDs with QD/SLHP composites are larger than those of LEDs with QD/SP composites. Thus, the conversion loss of QDs in LEDs with QD/SLHP composites is lower than that in LEDs with QD/SP composites even when equal proportions of QD light are generated. Moreover, these improvements can be larger at higher QD concentrations. This further supports the hypothesis that SLHP composites lead to less surface defects when a greater amount of QDs transfer from solution to polymer matrix. Especially at the high CCEs, ranging from 40% to 60%, that are generally used in white LEDs [30,31,35], their total radiant power and luminous flux can increase by 11.8% and 13.0%, respectively, compared with those using QD/SP composites, achieving a high luminous efficacy of 89.6 lm/W even at a large injection current of 0.19 A. Please note that such

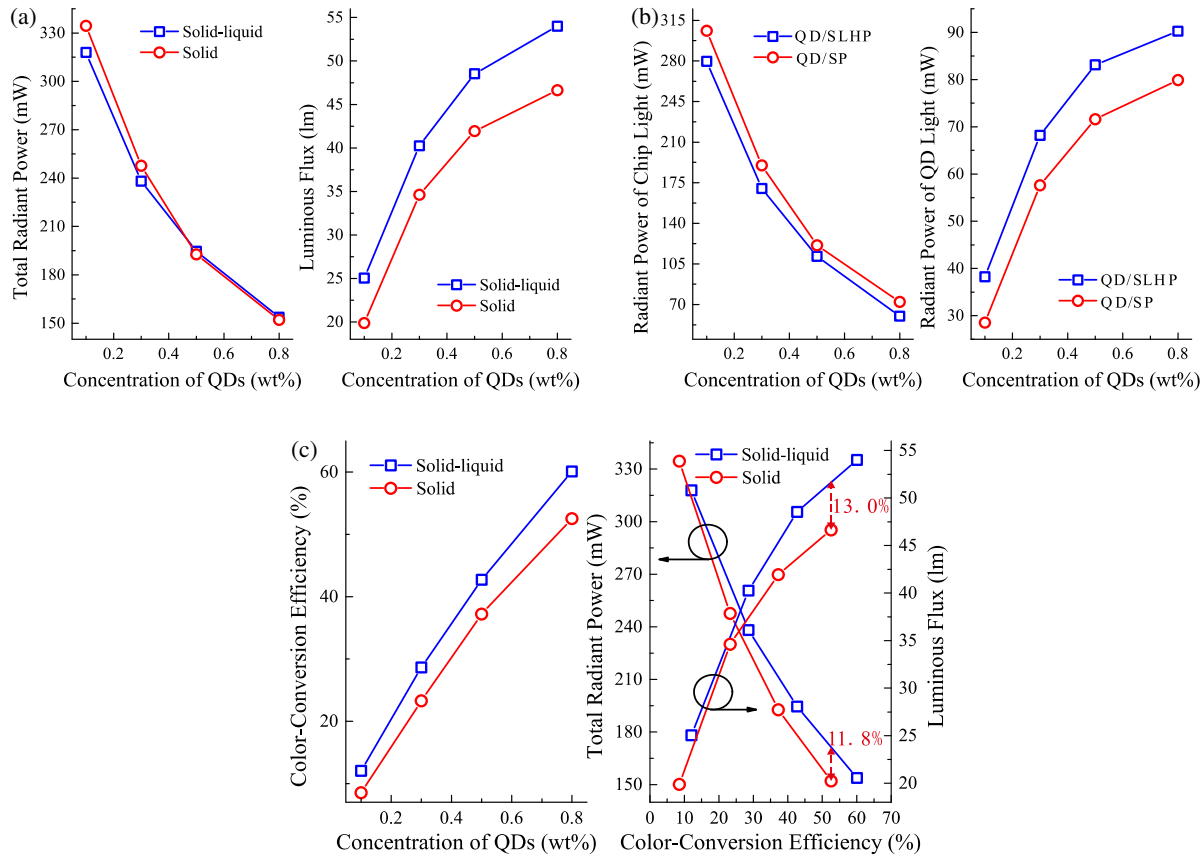

Fig. 7. (a) Total radiant power, luminous flux, (b) radiant power of chip light, and radiant power of QD light of LEDs with QD/SLHP composites and QD/SP composites at different QD concentrations. (c) CCE of LEDs with QD/SLHP composites and QD/SP composites at different QD concentrations; their total radiant power and luminous flux for different CCEs.

an efficiency is larger than previous reported QD-LEDs using green QDs as the only color convertor with solid-state packaging structures (~80 lm/W) [35,42,43], and comparable with that using liquid-state packaging structures (~105 lm/W) [35]. Therefore, the new approach of solid–liquid hybrid state shows great potential in achieving a high efficiency light source.

In addition, the spectra of LEDs with QD/SLHP and QD/SP composites are shown in Figs. 8(a) and 8(b), respectively. The intensity of the chip spectra (400 nm–500 nm) of QD/SLHP composites is lower than that of QD/SP composites at different QD concentrations, whereas it is the opposite for the intensity in the QD spectra (500 nm–600 nm). Besides, a redshift can be observed in the QD spectra with increasing QD concentration, which is generally regarded as the result of energy loss induced by QD aggregations and reabsorptions [44,45]. Most importantly, the peak wavelength and redshift are approximately equal for the two LED types when the QD concentration increases from 0.1 wt. % to 0.8 wt. %, as shown in the insets of the normalized spectra in Figs. 8(a) and 8(b), respectively. Therefore, the aggregation- and reabsorption-induced energy losses are not responsible for the improvement caused by SLHP composites.

B. Device Stability

The stability of LEDs with QD/SP composites and QD/SLHP composites were studied by aging tests. Both QD concentrations were kept at 0.6 wt. %, as shown in Fig. 9. Please note that two types of aging tests were carried out. First, an aging current of 0 mA (nonworking aging) was applied, which corresponds to LEDs without injection currents. Second, an aging current of 0.19 A (working aging) was applied; this is a harsh condition in studying the stability of QD-LEDs [13]. Both LEDs experienced a room temperature of 25°C without additional thermal management and were measured with a rating injection current of 0.19 A. For 0 mA, the luminous flux maintenance (LFM) of LEDs with QD/SLHP composites is obviously lower than that of LEDs with QD/SP composites at the same aging time because the dispersed QDs in the methyl-PDMS may be aggregated owing to sedimentation during usage. This is demonstrated in the insets in Fig. 9: deep-orange aggregation particles can be observed at the bottom of the QD/methyl-PDMS composites for hours. However, the LFM values of the two LED types are approximately equal for an aging current of 0.19 A. This is because the LEDs with QD/SLHP composites exhibit less surface defects on QDs, leading to lower thermal power generated by nonradiative recombinations and suppressed thermal quenching [46]. Moreover, since QDs possess an extremely low thermal stability [47], SLHP composites help increase the lifetime of QD-LEDs and neutralize the LFM reduction caused by sedimentations. Consequently, SLHP composites can achieve high efficiency QD-LEDs without sacrificing the

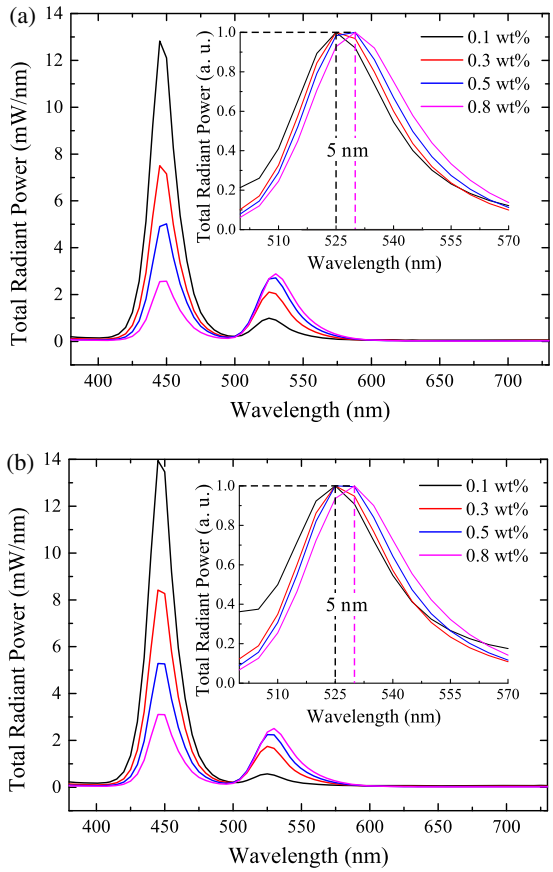

Fig. 8. Emission spectra of LEDs with (a) QD/SLHP composites and (b) QD/SP composites at different QD concentrations.

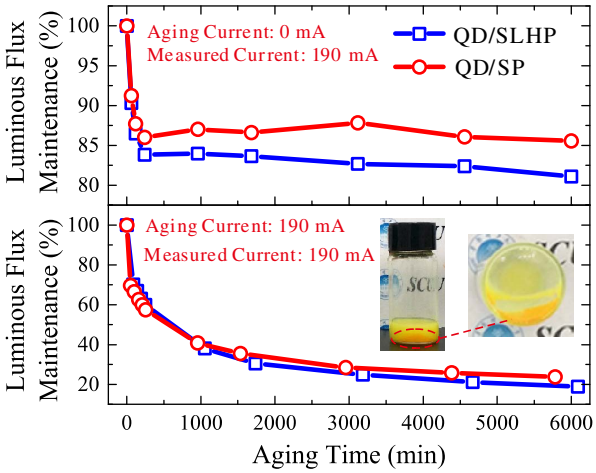

Fig. 9. LFM of LEDs with QD/SLHP composites and QD/SP composites after nonworking aging (aging current of 0 A) and working aging with a harsh condition (aging current of 0.19 A); the QD concentration is kept at 0.6 wt. %.

LFM after working aging compared with traditional SP composites, which is essential for their mass productions and commercial applications.

5. CONCLUSIONS

We propose a high efficiency solid–liquid hybrid-state QD-LED device; SLHP composites are used as dispersion matrices for QDs. The infrared transmittance spectra prove that ethylene-PDMS interacts with the curing agent after a heat treatment and creates a solid-state cross-linked network, which can store liquid methyl-PDMS. On a macroscopic level, the SLHP composites appear in a solid state after curing and can therefore be directly employed in current structures for illumination and display applications. Simultaneously, they own a liquid state from a microcosmic level, which provides a liquid environment for dispersing QDs. The results indicate that LEDs with QD/SLHP composites can achieve better optical performances than LEDs with conventional QD/SP composites, in particular when a methyl-PDMS concentration of 85 wt. % is used, which is the maximum concentration that can ensure that the ethylene-PDMS is entirely cross-linked and solid. Spectral analyses of the LEDs reveal that reabsorption and aggregation loss show approximately no influence on the optical performances according to the redshift in the QD spectra. However, the absorption spectra of the QD/SLHP films and QD/SP films reveal that less surface defects exist on QDs in QD/SLHP films, confirmed by the lower absorption compared with that of QD/SP films for long-wavelength light.

Regarding the optical performances at CCEs ranging from 40% to 60% as generally used for white LEDs, the luminous flux of LEDs with QD/SLHP composites (85 wt. % methyl-PDMS) increases by 13.0% compared with those with QD/SP composites. As a result, a high luminous efficacy of 89.6 lm/W (0.19 A) was achieved for QD-LEDs using QDs as the only color convertor. Moreover, the working-aging tests at a harsh condition indicate that LEDs with QD/SLHP composites can achieve an LFM comparable to that of LEDs using QD/SP composites. This is because the lower thermal power generated in QD/SLHP composites with less nonradiative recombination events can better suppress the thermal quenching of QDs, thereby providing a working stability comparable with that using conventional solid-state packaging structures. Consequently, the novel approach shows great potential for high efficiency and high stability QD-LEDs by providing a solid–liquid hybrid-state environment for QDs. We believe that this study can provide a new prospective for high efficiency QD-LED design and make significant contributions to illumination and display applications.

Funding. National Natural Science Foundation of China (NSFC) (51735004, 51775199); Natural Science Foundation of Guangdong Province (2014A030312017); Science Technology Program of Guangdong Province (2016B010130001).

REFERENCES

1. X. Dai, Z. Zhang, Y. Jin, Y. Niu, H. Cao, X. Liang, L. Chen, J. Wang, and X. Peng, "Solution-processed, high-performance light-emitting diodes based on quantum dots," Nature **515**, 96–99 (2014).
2. P. Pust, P. J. Schmidt, and W. Schnick, "A revolution in lighting," Nat. Mater. **14**, 454–458 (2015).
3. I. Coropceanu and M. G. Bawendi, "Core/shell quantum dot based luminescent solar concentrators with reduced reabsorption and enhanced efficiency," Nano Lett. **14**, 4097–4101 (2014).

4. Y. Shirasaki, G. J. Supran, M. G. Bawendi, and V. Bulović, "Emergence of colloidal quantum-dot light-emitting technologies," Nat. Photonics **7**, 13–23 (2013).
5. T. T. Xuan, J. Q. Liu, R. J. Xie, H. L. Li, and Z. Sun, "Microwave-assisted synthesis of CdS/ZnS:Cu quantum dots for white light-emitting diodes with high color rendition," Chem. Mater. **27**, 1187–1193 (2015).
6. S. Jiao, Q. Shen, I. Moraseró, J. Wang, Z. Pan, K. Zhao, Y. Kuga, X. Zhong, and J. Bisquert, "Band engineering in core/shell ZnTe/CdSe for photovoltage and efficiency enhancement in exciplex quantum dot sensitized solar cells," ACS Nano **9**, 908–915 (2015).
7. A. B. Greytak, P. M. Allen, W. Liu, J. Zhao, E. R. Young, Z. Popović, B. Walker, D. G. Nocera, and M. G. Bawendi, "Alternating layer addition approach to CdSe/CdS core/shell quantum dots with near-unity quantum yield and high on-time fractions," Chem. Sci. **3**, 2028–2034 (2012).
8. A. Aboulaich, M. Michalska, R. Schneider, A. Potdevin, J. Deschamps, R. Deloncle, G. Chadeyron, and R. Mahiou, "Ce-doped YAG nanophosphor and red emitting $CuInS_2$/ZnS core/shell quantum dots for warm white light-emitting diode with high color rendering index," ACS Appl. Mater. Interfaces **6**, 252–258 (2013).
9. H. Lin, B. Wang, J. Xu, R. Zhang, H. Chen, Y. Yu, and Y. Wang, "Phosphor-in-glass for high-powered remote-type white AC-LED," ACS Appl. Mater. Interfaces **6**, 21264–21269 (2014).
10. B. Xie, R. Hu, and X. Luo, "Quantum dots-converted light-emitting diodes packaging for lighting and display: status and perspectives," J. Electron. Packag. **138**, 020803 (2016).
11. Z. Liu, S. Liu, K. Wang, and X. Luo, "Optical analysis of color distribution in white LEDs with various packaging methods," IEEE Photon. Technol. Lett. **20**, 2027–2029 (2008).
12. A. W. Norris, M. Bahadur, A. Zarisfi, J. S. Alger, and C. C. Windiate, "Silicone materials for LED packaging," Proc. SPIE **6337**, 63370F (2006).
13. S.-C. Hsu, Y.-H. Chen, Z.-Y. Tu, H.-V. Han, S.-L. Lin, T.-M. Chen, H.-C. Kuo, and C.-C. Lin, "Highly stable and efficient hybrid quantum dot light-emitting diodes," IEEE Photon. J. **7**, 1601210 (2015).
14. D. Gerion, F. Pinaud, S. C. Williams, W. J. Parak, D. Zanchet, S. Weiss, and A. P. Alivisatos, "Synthesis and properties of biocompatible water-soluble silica-coated CdSe/ZnS semiconductor quantum dots," J. Phys. Chem. B **105**, 8861–8871 (2001).
15. Y. H. Kim, J.-Y. Bae, J. Jin, and B.-S. Bae, "Sol-gel derived transparent zirconium-phenyl siloxane hybrid for robust high refractive index LED encapsulant," ACS Appl. Mater. Interfaces **6**, 3115–3121 (2014).
16. J. Lee, V. C. Sundar, J. R. Heine, M. G. Bawendi, and K. F. Jensen, "Full color emission from II-VI semiconductor quantum dot-polymer composites," Adv. Mater. **12**, 1102–1105 (2000).
17. X. Wang, X. Yan, W. Li, and K. Sun, "Doped quantum dots for white-light-emitting diodes without reabsorption of multiphase phosphors," Adv. Mater. **24**, 2742–2747 (2012).
18. J. S. Li, Y. Tang, Z.-T. Li, X.-R. Ding, L.-S. Rao, and B.-H. Yu, "Effect of quantum dot scattering and absorption on the optical performance of white light-emitting diodes," IEEE Trans. Electron Devices **65**, 2877–2884 (2018).
19. M. Noh, T. Kim, H. Lee, C. K. Kim, S. W. Joo, and K. Lee, "Fluorescence quenching caused by aggregation of water-soluble CdSe quantum dots," Colloids Surf. A **359**, 39–44 (2010).
20. X. Li, Y. Liu, X. Song, H. Wang, H. Gu, and H. Zeng, "Intercrossed carbon nanorings with pure surface states as low-cost and environment-friendly phosphors for white-light-emitting diodes," Angew. Chem. Int. Ed. **54**, 1759–1764 (2014).
21. R. Lesyuk, B. Cai, U. Reuter, N. Gaponik, D. Popovych, and V. Lesnyak, "Quantum-dot-in-polymer composites via advanced surface engineering," Small Methods **1**, 1700189 (2017).
22. L. Kong, L. Zhang, Z. Meng, C. Xu, N. Lin, and X. Liu, "Ultrastable, highly luminescent quantum dot composites based on advanced surface manipulation strategy for flexible lighting-emitting," Nanotechnology **29**, 315203 (2018).
23. L. Ma, W. Xiang, H. Gao, L. Pei, X. Ma, Y. Huang, and X. Liang, "Carbon dot-doped sodium borosilicate gel glasses with emission tunability and their application in white light emitting diodes," J. Mater. Chem. C **3**, 6764–6770 (2015).
24. J. Jang, S. Kim, and K. J. Lee, "Fabrication of CdS/PMMA core/shell nanoparticles by dispersion mediated interfacial polymerization," Chem. Commun. **26**, 2689–2691 (2007).
25. W. Zhang, S. F. Yu, L. Fei, L. Jin, S. Pan, and P. Lin, "Large-area color controllable remote carbon white-light light-emitting diodes," Carbon **85**, 344–350 (2015).
26. Y. T. Kwon, N. S. Eom, Y. M. Choi, B. S. Kim, T. S. Kim, C. G. Lee, K. J. Lee, and Y. H. Choa, "Improvement of dispersion stability and optical properties of CdSe/ZnSe structured quantum dots by polymer coating," J. Nanosci. Nanotechnol. **14**, 7636–7640 (2014).
27. R. Liang, D. Yan, R. Tian, X. Yu, W. Shi, C. Li, M. Wei, D. G. Evans, and X. Duan, "Quantum dots-based flexible films and their application as the phosphor in white light-emitting diodes," Chem. Mater. **26**, 2595–2600 (2014).
28. J. S. Li, Y. Tang, Z.-T. Li, Z. Li, X.-R. Ding, and L.-S. Rao, "Investigation of the emission spectral properties of carbon dots in packaged LEDs using TiO_2 nanoparticles," IEEE J. Sel. Top. Quantum Electron. **23**, 2000507 (2017).
29. S. D. Yu, Y. Tang, Z. T. Li, K. H. Chen, X. R. Ding, and B. H. Yu, "Enhanced optical and thermal performance of white light-emitting diodes with horizontally layered quantum dots phosphor nanocomposites," Photon. Res. **6**, 90–98 (2018).
30. Y. Tang, Z. Li, Z. T. Li, J. S. Li, S. D. Yu, and L. S. Rao, "Enhancement of luminous efficiency and uniformity of CCT for quantum dot-converted LEDs by incorporating with ZnO nanoparticles," IEEE Trans. Electron Devices **65**, 158–164 (2018).
31. S. Yu, B. Zhuang, J. Chen, Z. Li, L. Rao, B. Yu, and Y. Tang, "Butterfly-inspired micro-concavity array film for color conversion efficiency improvement of quantum-dot-based light-emitting diodes," Opt. Lett. **42**, 4962–4965 (2017).
32. F. Li, X. Wang, Z. Xia, C. Pan, and Q. Liu, "Photoluminescence tuning in stretchable PDMS film grafted doped core/multishell quantum dots for anticounterfeiting," Adv. Funct. Mater. **27**, 1700051 (2017).
33. K. T. Shimizu, M. Böhmer, D. Estrada, S. Gangwal, S. Grabowski, H. Bechtel, E. Kang, K. J. Vampola, D. Chamberlin, and O. B. Shchekin, "Toward commercial realization of quantum dot based white light-emitting diodes for general illumination," Photon. Res. **5**, A1–A6 (2017).
34. T. L. Shen, K. J. Chen, C. W. Sher, H. V. Han, K. Y. Wang, J. R. Li, C. C. Lin, M. H. Shih, C. C. Fu, and H. C. Kuo, "High quality liquid-type quantum dots white light-emitting diode," Nanoscale **8**, 1117–1122 (2016).
35. S. Sadeghi, B. G. Kumar, R. Melikov, M. M. Aria, H. B. Jalali, and S. Nizamoglu, "Quantum dot white LEDs with high luminous efficiency," Optica **5**, 793–802 (2018).
36. H. W. Chen, R. D. Zhu, J. He, W. Duan, W. Hu, Y. Q. Lu, M. C. Li, S. L. Lee, Y. J. Dong, and S. T. Wu, "Going beyond the limit of an LCD's color gamut," Light Sci. Appl. **6**, e17043 (2017).
37. A. C. C. Esteves, J. Brokken-Zijp, J. Laven, H. P. Huinink, N. J. W. Reuvers, M. P. Van, and G. D. With, "Influence of cross-linker concentration on the cross-linking of PDMS and the network structures formed," Polymer **50**, 3955–3966 (2009).
38. K.-J. Chen, H.-V. Han, H.-C. Chen, C.-C. Lin, S.-H. Chien, C.-C. Huang, T.-M. Chen, M.-H. Shih, and H.-C. Kuo, "White light emitting diodes with enhanced CCT uniformity and luminous flux using ZrO_2 nanoparticles," Nanoscale **6**, 5378–5383 (2014).
39. L. Hartmann, A. Kumar, M. Welker, A. Fiore, C. Julien-Rabant, M. Gromova, M. Bardet, P. Reiss, P. N. W. Baxter, F. Chandezon, and R. B. Pansu, "Quenching dynamics in CdSe nanoparticles: surface-induced defects upon dilution," ACS Nano **6**, 9033–9041 (2012).
40. A. Cretí, M. Anni, M. Z. Rossi, G. Lanzani, G. Leo, F. Della Sala, L. Manna, and M. Lomascolo, "Ultrafast carrier dynamics in core and core/shell CdSe quantum rods: role of the surface and interface defects," Phys. Rev. B **72**, 125346 (2005).
41. J. Li, Y. Tang, Z. Li, K. Cao, C. Yan, and X. Ding, "Full spectral optical modeling of quantum-dot-converted elements for light-emitting diodes considering reabsorption and reemission effect," Nanotechnology **29**, 295707 (2018).
42. X. Yuan, R. Ma, W. Zhang, J. Hua, X. Meng, X. Zhong, J. Zhang, J. Zhao, and H. Li, "Dual emissive manganese and copper Co-doped

Zn-In-S quantum dots as a single color-converter for high color rendering white-light-emitting diodes," ACS Appl. Mater. Interfaces **7**, 8659–8666 (2015).
43. S. H. Park, A. Hong, J. H. Kim, H. Yang, K. Lee, and H. S. Jang, "Highly bright yellow-green-emitting $CuInS_2$ colloidal quantum dots with core/shell/shell architecture for white light-emitting diodes," ACS Appl. Mater. Interfaces **7**, 6764–6771 (2015).
44. W. Zhang, D. Dai, X. Chen, X. Guo, and J. Fan, "Red shift in the photoluminescence of colloidal carbon quantum dots induced by photon reabsorption," Appl. Phys. Lett. **104**, 091902 (2014).
45. Y. Li, H. Lin, C. Luo, Y. Wang, C. Jiang, R. Qi, R. Huang, J. Travas-sejdic, and H. Peng, "Aggregation induced red shift emission of phosphorus doped carbon dots," RSC Adv. **7**, 32225–32228 (2017).
46. J. Y. Woo, K. N. Kim, S. Jeong, and C.-S. Han, "Thermal behavior of a quantum dot nanocomposite as a color converting material and its application to white LED," Nanotechnology **21**, 495704 (2010).
47. B. Xie, H. Liu, R. Hu, C. Wang, J. Hao, K. Wang, and X. Luo, "Targeting cooling for quantum dots in white QDs-LEDs by hexagonal boron nitride platelets with electrostatic bonding," Adv. Funct. Mater. **28**, 1801407 (2018).